Chapter 5

Motional Systematic Effects

5.1 Introduction

Precision measurements in general and electron electric dipole moment experiments in particular are extended exercises in controlling systematic effects. Section 3.5 describes the origin, size, and some manifestations of motional magnetic field effects, and describes in general terms the application of electric field quantization to suppress them. Section 2.6 discusses the fifty-year history of confronting them. Because control of the motional magnetic field effects is central to the experiment, Ulrich Jentschura and Benedikt Wundt joined with Charles Munger to publish a full calculation ("Quantum Dynamics in Atomic-Fountain Experiments for Measuring the Electric Dipole Moment of the Electron with Improved Sensitivity") in Physical Review X 2, 041009 (2012), an open access journal. The paper runs 25 pages with a supplemental ten page addition. Prof. Jentschura remains as a collaborator. The material in this chapter is largely complementary to those papers with its emphasis on the implementation of the electric field quantization method.

We examine the evolution of an atom in a strict fountain, in which the atoms rise and fall along a single line in the symmetry plane of the electric field plates and so the electric field, while it may vary in magnitude, is uniform in direction[1]. When the zero of time is set at the apogee of the atomic trajectory,

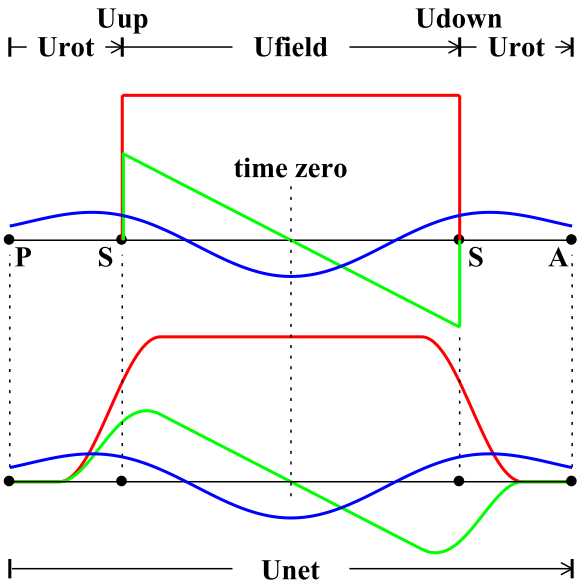

Figure 5.1: The upper figure illustrates the fields when the electric field is approximated as a step function. The lower figure illustrates the typical time dependence of fields applied to the atom as it enters between electric field plates, reverses under gravity, and exits; the duration of the transition region from zero to full electric field has been exaggerated for clarity. The electric field is shown in red, the motional magnetic field in green, and a plausible example of the static magnetic field in blue. The lower half of the figure illustrates the fields when the electric field is approximated as a step function.

[1] What if the electric field plates while symmetric about a symmetry plane are not quite flat, so that the electric field, even if it is uniform in direction, is not quite uniform in magnitude? There exists (unpublished work by collaborator Charles T. Munger) a transformation of variables that yields an equivalent problem where the electric field is exactly constant, the time symmetry of the fields experienced by the atom from transformed motional and from transformed static magnetic fields is preserved, and the values of the integrals of Eq. (5.13) are also preserved. All the cancellations work; the only change will be a negligible change in scale of D in Eq. (5.12), so our observable will still be nonzero only if an electron EDM exists.

then in the rest frame of the atom the electric field that the atom experiences is an even function of time; the magnetic field (motional magnetic field) due to the atom's motion through the electric field is an odd function of time; and the magnetic field due to the atom's motion though static laboratory magnetic fields is an even function of time.

The time dependence of the fields as the atoms rise between and fall out of the electric field plates is indicated in the lower half of Fig. 5.1. As a result of the application of these fields, the atomic state of an atom as it transits from the time and point of state preparation at the point P, to the time and point of state analysis at the point A, undergoes a complicated unitary transformation $U_{\rm net}$ that mixes states of the upper hyperfine level.

The unitary transformation $U_{\rm net}$ can be found by solving numerically the Schrödinger equation for the interaction of the $2F + 1 = 11$ states of the $F = 5$ hyperfine level, given prescribed magnetic fields in the x, y, and z directions, and an electric field in the z direction, where all the fields are functions of time. This is certainly an excellent way to check that a scheme to extract an electron EDM, once known, indeed eliminates systematic errors. The sheer complexity of the problem makes such a numerical solution almost useless for finding an acceptable scheme in the first place. It is much better to decompose $U_{\rm net}$ into a product of five simpler pieces, as is illustrated in the upper half of Fig. 5.1.

The upper half of the figure shows the approximation generated when the electric field is taken to have a step-function rise at S chosen such that the assumed constant value of the square of the electric field E times the time within the step-function field, and the time integral $\int E^2\,dt$ of the actual field, are the same. The net unitary transformation is a product of distinct pieces: a rotation $U_{\rm rot}$ by static magnetic fields, only; a transformation $U_{\rm field}$ where the electric field is constant; and two transformations $U_{\rm up}$ and $U_{\rm down}$ that provide the corrections for the ramp-up and ramp-down of the electric field taking a finite amount of time.

In more detail: in an atomic fountain, the electric field applied to the atoms starts at zero, ramps over a finite time to a constant value, and ramps back to zero; the duration of the ramps is a small fraction of the time the atoms spend in the full field. We imagine for simplicity this ramp is squared off, so that the electric field jumps from zero to its full value, and from full value back to zero, at times indicated by S; we defer for a moment how one should best choose S. Since the electric field is now zero from P to S, and again from S to A, the motional magnetic field is now also zero there, and so the motional magnetic field now also jumps discontinuously at S. One can now solve for the unitary transformation within the electric field with the electric field constant, which is a great simplification; this transformation is $U_{\rm field}$.

Outside the electric field, from P to S and from S to A, there is no electric field and so no motional magnetic field; there are only the remnant magnetic fields encountered by the atom along its trajectory. The effect of these fields applied from P to S only causes some rotation of the atom, and so is simple to describe; the identical rotation occurs again from S to A. Thus if we can tune the static fields outside the electric-field region so that net rotation is zero, we would have

$$U_{\rm net} \sim U_{\rm field}\ , \tag{5.1}$$

and in the presence of a net rotation we have instead the better approximation

$$U_{\rm net} \approx U_{\rm rot} U_{\rm field} U_{\rm rot}\ ; \tag{5.2}$$

both approximations are valid only to the extent that the effects of the finite duration of the ramping of the electric field is ignored.

We include the finite duration of the ramping by inserting a unitary operator, to be applied at the time S, that gives the correction for the finite duration; the corrections $U_{\rm up}$ and $U_{\rm down}$, to be applied when the atom enters and leaves the electric field, respectively, are different. A careful choice of the precise point S allows these corrections to correct the difference in motion of the atom with and without a finite duration of the ramp. With these corrections we have the *exact* equality

$$U_{\rm net} = U_{\rm rot} U_{\rm down} U_{\rm field} U_{\rm up} U_{\rm rot}\ . \tag{5.3}$$

Each of these simpler transformations can be computed as a convergent series in a small parameter: for $U_{\rm rot}$ that parameter is the small angle of rotation; for $U_{\rm field}$ the small parameter is the ratio $1/\mu \sim 5 \times 10^{-3}$ that is (roughly speaking) the ratio for atoms in the electric field of the energy shifts due the Zeeman effect to those due to the tensor Stark effect (See Eq. D.5); and for $U_{\rm up}$ and $U_{\rm down}$ the small parameter of order $\sim 1 \times 10^{-2}$ is the ratio of the time spent in the ramp-up region to the total time spent in the electric field. Therefore the product $U_{\rm net}$ can also be computed as a series in small parameters; and it becomes possible to devise an e-EDM measurement in which sources of systematic error, term by term in the small parameters, are either made to cancel or can be measured and tuned to be negligible.

In the following three sections we describe in turn how to generate the series for $U_{\rm field}$; then for $U_{\rm rot}$; and then for $U_{\rm up}$ and $U_{\rm down}$. Each of these separate unitary transformations is unity to leading order; in each section we will discuss how to deal with the systematic errors in the electron EDM that would arise if the other transformations were exactly unity, that is, if we had respectively

$$U_{\rm net} \approx U_{\rm field} \tag{5.4}$$

or

$$U_{\rm net} \approx U_{\rm rot} U_{\rm rot} \tag{5.5}$$

or

$$U_{\rm net} \approx U_{\rm down} U_{\rm up} \tag{5.6}$$

Then in section 5.6 we describe how to adjust an atomic fountain to eliminate systematic errors in an actual electron EDM experiment when all the sources of systematic error are present at once and interact, using the full expression of Eq. (5.3).

5.2 Motional Systematic Effects in the Electric Field Region

5.2.1 Computation of $U_{\rm field}$

The detailed atomic theory of the time-evolution of an alkali-atom ground state in a constant electric but variable magnetic field has been presented in reference [WMJ12].

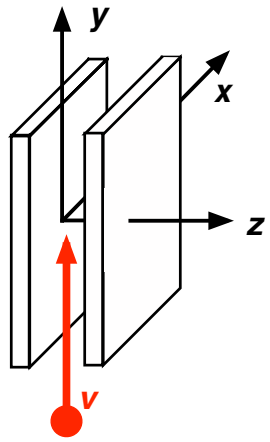

Figure 5.2: The coordinates used to describe the atomic fountain. The atom (red dot) moves up and down the y axis. The electric field is perpendicular to the atomic motion and is directed along the z axis; the motional magnetic field is therefore parallel to the x axis.

The coordinate system that we shall use to describe the atom is shown in Fig. 5.2 and follows from Fig. 3.1a. The y axis is vertical, and atoms in the fountain rise and fall along the y axis. The electric field applied, however it may vary in magnitude, is constant in direction and is horizontal and defines the z axis; this axis is used as the quantization axis to describe the atomic states. The motional magnetic field is therefore constrained to be horizontal and its direction is parallel to the x axis.

The time evolution of an atom in the upper ground-state hyperfine level is governed by an effective Hamiltonian; dropping terms that contribute an irrelevant global phase common to all states in the level, that effective Hamiltonian can be written as

$$H = A_{\rm S}\, \mathbf{F}_z^2\, E_z^2 + \mu_B\, g_F\, \mathbf{F} \cdot \vec{B} - R\, d_{\rm e}\, \frac{\mathbf{F}_z}{F}\, E_z\,. \tag{5.7}$$

where $\mathbf{F}$ is the total angular momentum[2]. The first term is due to the tensor Stark effect (See

[2]The symbol $\mathbf{F}$ is used for the value of $\vec{F}/\hbar$, where $\vec{F}$ is the angular momentum with units of $\hbar$; thus for integer total spin F the quantity $\mathbf{F}_z$ is a diagonal matrix whose diagonal elements from top left to bottom right are the integers F, $F-1$, ..., $-F$.

Section 3.4), which splits levels of different values of $|M|$ by an amount quadratic in the electric field E_z; for ^{211}Fr we have $A_S = 3.61 \times 10^{-46}\,\mathrm{J/(V/m)^2}$ [DFBD10].

The second term is due to the Zeeman effect from the magnetic fields $\vec{B}$ experienced by the atom in its rest frame; these fields are the sum of motional magnetic field ($\vec{B}_{\mathrm{mot}} = \vec{v} \times \vec{E}/c^2$) due to the atom's motion through the applied electric field, and fields due to the atom's motion through stray static laboratory magnetic fields. In Eq. (5.7), the parameter μ_B is the Bohr magneton, and for ^{211}Fr in the $F = 5$ hyperfine level the Landé g-factor is $g_F = 0.2$. The last term in the Hamiltonian describes the effect of an electron electric dipole moment d_e; here R is the enhancement factor (See Section 2.3). Contributions to the effective Hamiltonian from the mixing of the ground-state hyperfine levels, or from terms in the Stark effect of order E_z^4, are negligible.

We begin by examining an electron EDM experiment in the case where the electric field makes a step-function rise from zero to a constant value, and where remnant magnetic fields are negligible (may be taken to drop sharply to zero) outside the electric field region. The typical time-dependence of the fields applied to the atom in a practical atomic fountain is illustrated in Fig. 5.3. The electric field is constant; with the zero of time set at the apogee of the atomic trajectory, the electric field is an even function of time.

The motional magnetic field is an odd function of time (given the parabolic rise and fall of an atom under gravity, in fact a linear function of time); the magnetic fields experienced by the atom due to its motion through remnant magnetic fields are even functions of time. The magnitude of the magnetic fields can be reduced to less than 200 fT and quite possibly less than 20 fT (Section 5.5) by a combination of magnetic shielding, shield demagnetization, and nulling of remnant magnetic fields and gradients.

In an electric field the tensor Stark effect causes an oscillation in phase of the amplitude for a state to be in a state $|F, M\rangle$ compared to another such state $|F, M'\rangle$ with $|M| \neq |M'|$. The square inset in Fig. 5.3 shows for ^{211}Fr the time dependence of

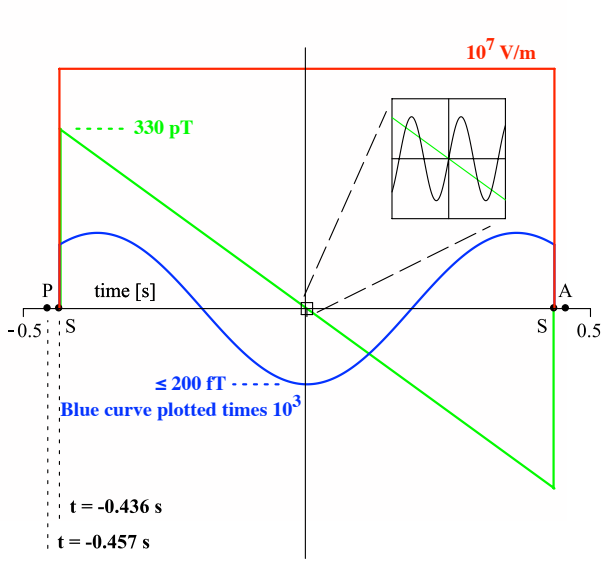

Figure 5.3: Plot as a function of time of the electric and magnetic fields experienced in the rest frame of an atom of ^{211}Fr in an atomic fountain in the approximation that the time evolution is given entirely by U_{field}. The electric field E_z is shown in red; the motional magnetic field is shown in green; and the magnetic field seen by the atom in its transit through static but spatially varying laboratory magnetic fields is shown in blue. Shown in black, in the insert (at $10\times$ scale) is the phase of the state $|51\rangle$ relative to the state $|50\rangle$.

the *slowest* such change in phase, that between the states $|50\rangle$ and the states $|5, \pm 1\rangle$. As the figure shows, the period of even this oscillation is very much shorter than the typical time over which any magnetic field encountered by the atom changes; the period of the oscillation between states of large magnetic quantum number is shorter still (by a factor of $5^2 - 4^2 = 9$ for the states $|55\rangle$ and $|54\rangle$, for example). Integrals that arise in time-dependent perturbation theory whose integrands involve the product of the magnetic fields applied to the atom and such an oscillating phase will be small.

It is convenient to adopt a system of dimensionless units used in Ref. [WMJ12], where we use a dimensionless variable t that is proportional to time, such that the step-function up in the electric field occurs at $t = -\tau$, and the step-function down occurs at $t = +\tau$, where $\tau = 1/2$. This can be accom-

plished by defining an electric field scale

$$E_S = \sqrt{\frac{\hbar}{T\,A_{\rm S}}}\,, \tag{5.8}$$

where $T = 0.67\,\mathrm{s}$ is the total time spent in the electric field; the dimensionless Schrödinger equation to be solved for the unitary time evolution operator is

$$HU = i\frac{\partial U}{\partial t}\ , \tag{5.9}$$

where the boundary condition is $U(-\tau) = 1$, and

$$H(t) = \epsilon_z^2(t)\,\mathbf{F}_z^2 + \vec{\beta}(t)\cdot\mathbf{F} + \sigma_F\,\epsilon_z(t)\,\mathbf{F}_z\,. \tag{5.10}$$

Here all quantities are dimensionless:

$$\epsilon_z = \frac{E_z}{E_S}\,;\quad \vec{\beta} = \frac{g_F\,\mu_B\,\vec{B}}{A_{\rm S}\,E_S^2}\,;\quad \text{and } \sigma_F = -\frac{d_{\rm e}\,R}{F\,A_{\rm S}\,E_S}\,. \tag{5.11}$$

The first quantity measures the strength of the electric field; the second, the strength and direction of the magnetic field; the last the strength of the electron EDM; and as before, for ^{211}Fr we have $A_{\rm S} = 3.61\times10^{-46}\,\mathrm{J/(V/m)^2}$ [DFBD10].

Under the conditions of our experiment we have that the quantity

$$D \equiv -\sigma_F\int_{-\tau}^{\tau}\epsilon_z(t)\,dt\ , \tag{5.12}$$

which equals the angle ^{211}Fr atom rotates due to the interaction of the electron EDM and the applied electric field, has for $d_{\rm e} = 1.3\times10^{-50}$ a magnitude of 1.5×10^{-7} radians.

The quantity $\vec{\beta}$ measures the vector magnetic field; the units of magnetic field is the rotation angle, in radians, if a constant field $\vec{\beta}$ were applied to the atom in free space for a time T equal to the time spent in the electric field. For a average remnant magnetic field of 200 fT that angle is 2.5×10^{-3} radians, while if the maximum motional magnetic field were applied for that same amount of time the angle would be 3.9 radians.

We have already described in Section 3.7.3 how the design of an experiment to measure an electron EDM leads naturally to imposing the conditions that the Stark and Zeeman phases accumulated by the atoms due to fields in the z directions shall be set to integer multiples of π. In our dimensionless units, the conditions of Eq. (3.51) and Eq. (3.43) take the form:

$$\begin{aligned}\int_{-\tau}^{\tau}\epsilon_z^2(t)\,dt &= k_\epsilon\pi\\ \int_{-\tau}^{\tau}\beta_z(t)\,dt &= k_\beta\pi\end{aligned} \tag{5.13}$$

where k_ϵ and k_β are integers.

When $k_\epsilon + k_\beta$ is even, this pair of conditions has the physical interpretation that in the absence of any transverse magnetic fields (and any electron EDM) that an atom that enters the electric field in any superposition of magnetic sublevels $\big|5, M\big\rangle$ will exit in that same superposition, so that $U(\tau) = 1$. In practice we shall choose $k_\beta = 0$ (to keep all magnetic fields in the apparatus small) and $k_\epsilon = 66$.

With the phases so set, we have $U = VU_{\rm field}$, where for $k_\epsilon + k_\beta$ even we have $V = 1$. For $k_\epsilon + k_\beta$ odd we have $V = \exp(-i\pi\mathbf{F}_z)$, which is also a diagonal matrix, with elements that alternate between $+1$ and -1; for $F = 5$ we have

$$V = \mathrm{diag}\,\big(1,\,-1,\,1,\,-1,\,1,\,-1,\,1,\,-1,\,1,\,-1,\,1\big)\ . \tag{5.14}$$

In the absence of transverse magnetic fields ($\beta_x(t) = \beta_y(t) = 0$) we have $U_{\rm field} = 1$; in the presence of such fields $U_{\rm field}$ can be written as a perturbation series in powers of the transverse fields. The series is certain to converge, however large the transverse fields might be, because the size of the basis set of the problem we are solving, equal to the number $2F+1$ of states in the upper hyperfine level, is finite. We have the triple series [WMJ12]

$$\begin{aligned}U_{\rm field} - 1 = \\ \sum_{n=1}^{\infty}\sum_{k=\lceil n/2\rceil}^{\infty}\Bigg(\ &\frac{i^{n+k}}{\mu^k}\ \sum_j \mathcal{N}_{n,k}^{(j)}(F)\,\mathcal{G}_{n,k}^{(j)}(\vec{\beta}(t))\\ &+\frac{i^{n+k+1}}{\mu^k}\sum_j \mathcal{M}_{n,k}^{(j)}(F)\,\mathcal{B}_{n,k}^{(j)}(\vec{\beta}(t))\Bigg)\end{aligned} \tag{5.15}$$

In this expansion all the quantities are real except the explicit imaginary factors of i. The sum over n

represents the sum over the terms of n^{th} order in perturbation theory in powers of the transverse magnetic fields. Each of these terms in turn can be represented as an (in general asymptotic) series in powers k of the parameter $1/\mu$. The origin of this expansion lies in the rapidity with which the phases of the states $\left|F, M\right\rangle$ due to the tensor Stark effect change compared to the time scale over which the transverse magnetic fields change (Fig 5.3).

In terms of the time T spent in the electric field, the Stark shift, and the electric field, we have for the expansion parameter

$$\frac{1}{\mu} = \frac{\hbar}{T A_S E_Z^2} \approx 4.8 \times 10^{-3} \tag{5.16}$$

for ^{211}Fr held in an electric field of $9.56 \times 10^6\,\mathrm{V/m}$ for 0.67 s.

It is useful to represent the coefficient of each power of $1/\mu$ in Eq. 5.15 as a finite sum (indexed above by j) over a number of distinct convenient contributions. All 30 resulting terms of order up to and including $1/\mu^2$ have been calculated [WMJ12]; we remark that to obtain all these terms, it is necessary to carry out the perturbation expansion in powers of the transverse field out to fourth order, so the calculation is difficult. The quantities $\mathcal{N}$ and $\mathcal{M}$ are matrices of field-independent constants, which depend on the total spin F of the system under consideration; the quantities $\mathcal{G}$ and $\mathcal{F}$ are F-independent scalar functions of the applied magnetic field $\vec{\beta}$. All four quantities $\mathcal{N}$, $\mathcal{M}$, $\mathcal{G}$ and $\mathcal{F}$ have magnitudes of crude order unity for the fields in our apparatus; since for the atom ^{211}Fr the expansion parameter $1/\mu$ is small, the sum over powers of $1/\mu$ therefore converges rapidly.

Both the matrices $\mathcal{N}$ and $\mathcal{M}$, and both the scalars $\mathcal{B}$ and $\mathcal{G}$, in general depend on whether $k_\epsilon + k_\beta$ is even or odd. For example we have [WMJ12] the diagonal matrix

$$\mathcal{M}^{(1)}_{2,2}(5) = \mathrm{diag}\begin{pmatrix} -5/162 \\ -242/3969 \\ -363/2450 \\ -121/225 \\ -121/18 \\ 0 \\ 121/18 \\ 121/225 \\ 363/2450 \\ 242/3969 \\ 5/162 \end{pmatrix}, \tag{5.17}$$

and the pentadiagonal matrix:

$$\mathcal{M}^{(2)}_{2,2}(5) = \begin{pmatrix}
0 & 0 & \sqrt{5}/168 & & & & & & & & \\
0 & 0 & 0 & \sqrt{3}/35 & & & & & & & \\
\sqrt{5}/168 & 0 & 0 & 0 & \sqrt{42}/30 & & & & & & \\
 & \sqrt{3}/35 & 0 & 0 & 0 & \sqrt{210}/6 & & & & & \\
 & & \sqrt{42}/30 & 0 & 0 & 0 & 0 & & & & \\
 & & & \sqrt{210}/6 & 0 & 0 & 0 & -\sqrt{210}/6 & & & \\
 & & & & 0 & 0 & 0 & 0 & -\sqrt{42}/30 & & \\
 & & & & -\sqrt{210}/6 & 0 & 0 & 0 & -\sqrt{3}/35 & & \\
 & & & & & \sqrt{42}/30 & 0 & 0 & 0 & -\sqrt{5}/168 & \\
 & & & & & & -\sqrt{3}/35 & 0 & 0 & 0 & \\
 & & & & & & & -\sqrt{5}/168 & 0 & 0 &
\end{pmatrix} \tag{5.18}$$

The scalar factors that multiply these matrices are respectively

$$\mathcal{B}^{(1)}_{2,2} = -\int_{-\tau}^{\tau} z_e(t)\left[x_e^2(t) + x_o^2(t) + y_e^2(t)\right] dt + \begin{cases} -2\int_{-\tau}^{\tau} x_o'(t) y_e(t)\, dt & \text{for } k_\epsilon + k_\beta \text{ even}, \\ +2\int_{-\tau}^{\tau} x_o(t) y_e'(t)\, dt & \text{for } k_\epsilon + k_\beta \text{ odd}, \end{cases} \tag{5.19}$$

and

$$\mathcal{B}^{(2)}_{2,2} = x_o(-\tau) y_e(-\tau)\,. \tag{5.20}$$

In writing these scalar factors we have followed [WMJ12] and for simplicity denoted the components of the vector $\vec{\beta}(t)$ not as β_x and β_y, but merely as x and y, respectively; and separated the magnetic fields according to whether when the electric field changes sign the component reverses sign (subscript "o", for odd) or does not reverse sign

(subscript "e", for even). The scalar functions can depend on values of the magnetic field at a point just inside the electric field;for example we define:

$$x_o(-\tau) = \lim_{t\to 0^+} x_o(-\tau + t) \ . \tag{5.21}$$

The functions can also depend on integrals over fields (for example, $x_o(t)$) or their time-derivatives (like $x'_o(t)$).

Evaluating the effect of transverse fields is merely a matter of substituting the known series for U into the expression for an observable P.

To isolate an electron EDM the first observable to try would be that of the magnetometer illustrated in Fig. 3.11, which detects a small rotation of the atom about the z axis, since an electron EDM manifests itself as such a rotation that changes sign with the applied electric field. For this particular observable[3] P we have proved a very useful result, valid to all orders n in the transverse fields and for powers of $1/\mu$ arbitrarily high:

> The series expansion of P has only even powers of $1/\mu$. (5.22)

Since in the proposed experiment for ^{211}Fr , we have $1/\mu^2 \approx 2\times 10^{-5}$, and since we are looking for an effect of order $|D| \approx 3\cdot 10^{-7}$, uncalculated terms of order $1/\mu^4$ will be numerically negligible and only the few terms in P of order $1/\mu^2$ need to be taken into account.

For a system where the total spin F of the upper hyperfine level is even (such as for ^{133}Cs, where $F=4$) this observable suffices and there are but two contributions at order $1/\mu^2$ to deal with. For ^{211}Fr where the total spin is odd, the number doubles inconveniently to four. This doubling can be traced to the rotated state $R_y(\pi/2)\big|F,0\big\rangle$ having only even-M components if F is even, and having only odd-M components if F is odd. Because the states $\big|F,1\big\rangle$ and $\big|F,-1\big\rangle$ mix at second order in the transverse magnetic fields, two extra systematics appear at order $1/\mu^2$ when F is odd.

However by altering the angle of propagation of the laser that prepares the initial state, the amplitude for being in either of the states $\big|F,\pm 1\big\rangle$ can be made zero even when F is odd, and the number of contributions to one systematic error can be lowered again to two (see also Section 3.7.5).

The altered initial states $R_y(\pi/2\pm\lambda)\big|50\big\rangle$ have zero amplitude for being in either of the degenerate states $\big|5,\pm 1\big\rangle$ for two different angles λ, of which the most sensitive to an electron EDM is

$$\lambda = \arccos\Big(\frac{1}{21}\sqrt{294+42\sqrt{7}}\Big) \approx 0.2892\,\text{radian} \ . \tag{5.23}$$

The pattern of lasers[4] required to generate an observable that uses such initial states is displayed in Fig. 5.4.

[3] An atom initially in a state ψ that is a coherent superposition of hyperfine levels,

$$\psi = \sum_{M=-F}^{F} a_M\big|5M\big\rangle \ ,$$

where the constants a_M are complex amplitudes, will end in the upper hyperfine level with a probability

$$P = \sum_{M=-5}^{5} c_M\big|\big\langle 5M|\psi\big\rangle\big|^2 \ .$$

If the axis of linear polarization of the state preparation laser is rotated to be $R_1\hat{z}$ while that of the analysis laser is rotated to be $R_2\hat{z}$, and if between the application of the state preparation laser and of the analysis laser the atom evolves within the $F=5$ hyperfine manifold according to some unitary operator U, then the resulting probability for the atom to remain in the upper hyperfine level is

$$P = \sum_{M=-5}^{5} c_M\big|\big\langle 5M\big|R_2^\dagger U R_1\big|50\big\rangle\big|^2 \ .$$

[4] In Fig. 5.4 the state preparation laser propagates vertically. But the only requirement to make the system work is to have the axis of linear polarization in the x-z plane and making angles $\pm\lambda$ with respect to the z axis. One could accomplish that by having lasers that propagate instead in the horizontal x-z plane, where one propagates with its axis of propagation making an angle $-\lambda$ with respect to the x axis, and the other propagates with its axis of propagation making an angle $+\lambda$ with respect to the x axis. Since $|\lambda|$ is small, the most of the heating is parallel to the electric field plates, which is acceptable. The lasers would now propagate in the horizontal plane, which may be experimentally more convenient. We can choose whichever geometry works best in practice.

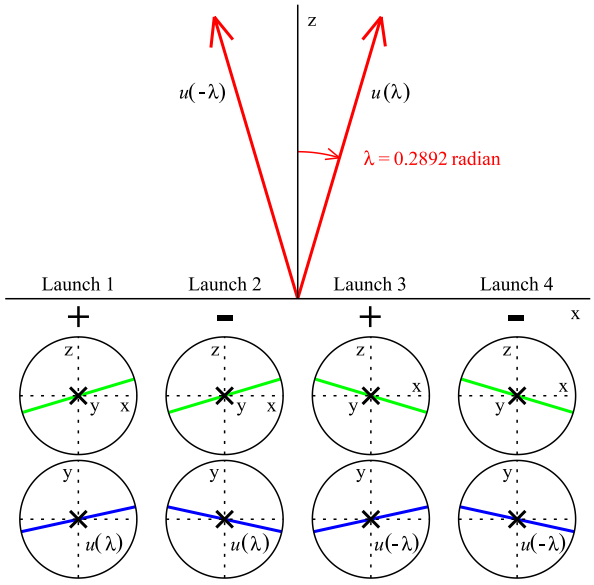

Figure 5.4: The pattern of laser polarizations for four consecutive launches required to reduce the number of systematic effects for $F = 5$ from four, typical for F odd due to the presence of $|M| = 1$, to two. The number of steps doubles because each step is done for two orientations of the laser (λ and $-\lambda$). In this implementation, the preparation laser propagates vertically (parallel to y) and the orientation of its laser polarization for each launch is shown in the upper circular inset in green. The analysis laser propagates in the horizontal plane either parallel to the direction $u(\lambda)$ or $u(-\lambda)$; the orientation of its laser polarization for each launch is shown in the lower circular inset in blue. The values of the observable P for each the four launches are combined with the signs shown.

The result is an observable that computes to

$$\boxed{P(\theta) = Dp_0 + \frac{1}{\mu^2}\left(\mathcal{B}^{(1)}_{2,2}p_1 + \mathcal{B}^{(2)}_{2,2}p_2\right) + O(1/\mu^4)\ ,} \tag{5.24}$$

where the first term contains the effect of the electron EDM via $D = -\sigma_F \epsilon_z$, and the coefficients $\mathcal{B}$ of the remaining two terms depend on the motional and remnant magnetic field applied to the atom and are defined in Eq. (5.19) and Eq. (5.20) and in Ref. [WMJ12]. The quantities p are known functions of the angle θ that gives the orientation of the axis of linear polarization of the analysis laser; explicitly:

$$p_j = 4\cos(\lambda)\sin(2\theta)\sum_{n=0}^{4} c_{jn}[\cos(2\theta)]^n\ , \tag{5.25}$$

where the c_{jn} are constants (See Appendix Eqs. (B.6) through (B.8)). The formulas of Eq. (5.24) (up to and including terms of order $1/\mu^2$) and of Eq. (5.25) have been verified using the computer algebra program Maple$^{\text{TM}}$.

5.2.2 Systematic Effects from U_{field}

We pause to consider just how remarkable Eq. (5.24) is.

> **We began with a tipped initial state where there are nonzero amplitudes to be in any of 9 of the possible 11 states $|5, M\rangle$. We evolved this state with a unitary operator whose expansion to order $1/\mu^2$ contained some 30 distinct terms; we squared the resulting amplitude, greatly increasing the complexity of the expression; and by combining data for different directions and angle of linear polarization of the preparation laser, and for different angle of linear polarization of the analysis laser, contrived to cancel all the terms, other than that of an electron EDM itself, that might appear out to order $1/\mu^2$, except two. But Eq. (5.24) is even more useful than that; for by the general theorem of Eq. (5.22), the terms in P at order $1/\mu^3$, all cancel, leaving the error in the expression of order $1/\mu^4$.**

To examine the size of the remaining systematics we will for convenience define

$$b_1 = \mathcal{B}^{(1)}_{2,2}/\mu^2 \qquad \text{and} \qquad b_2 = \mathcal{B}^{(2)}_{2,2}/\mu^2 \tag{5.26}$$

so that Eq. (5.24) takes the form

$$P(\theta) = Dp_0(\theta) + b_1 p_1(\theta) + b_2 p_2(\theta)\ . \tag{5.27}$$

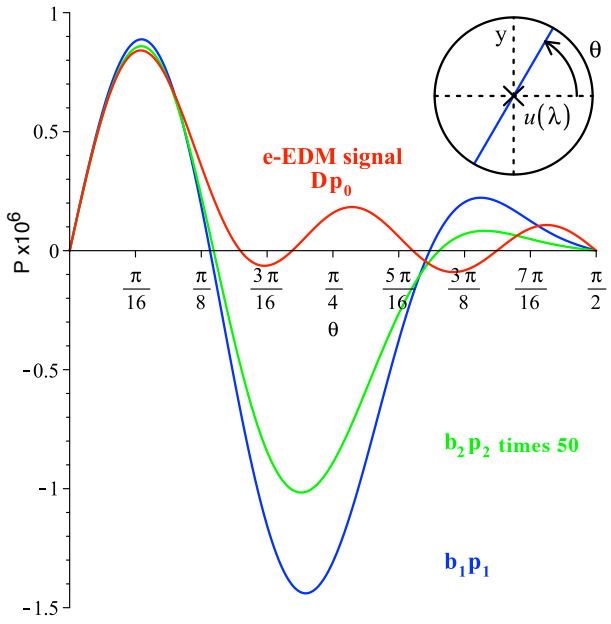

Figure 5.5: Plot of the contribution to P in Eq. (5.27) as a function of the angle θ of the linear polarization of the analysis laser; from an electron EDM of $1.3 \times 10^{-50}\,\mathrm{C\,m}$ (our experimental goal), and from the contributions of the two systematic errors $b_1 p_1$ and $b_2 p_2$ (scaled). The average vertical component of the magnetic field is set at 260 fT, so that the three functions are similar near the peak of the electron EDM signal near $\theta = \pi/16$.

The contributions to P from an electron EDM near the experimental goal and from the two surviving systematics, assuming an average vertical component of magnetic field of 260 fT, are plotted in Fig. 5.5 as a function of the angle θ of the linear polarization of the analysis beam.

The size of both systematics scales as the magnetic field component: larger or smaller magnetic fields will result in larger or smaller systematic terms. For the 260 fT chosen, the contribution from b_2 is already negligible for an experiment to improve the upper limit by a factor of 100. As it happens, b_2 depends linearly on $y_e(-\tau)$, the vertical component of the remnant magnetic field at a point just inside the electric field, and that parameter we will have to make a few hundred fT to avoid a systematic associated with the transition into the electric field. Therefore $\mathcal{B}^2_{2,2}$ will be effectively zero.

The remaining task is to reduce or cancel b_1 so that it is far below the electron EDM sensitivity.

Nulling the Vertical Magnetic Field

When $k_\epsilon + k_\beta$ is even, the part of $\mathcal{B}^1_{2,2}$, and so of b_1, that is odd in the electric field, is from Eq. (5.19) proportional to the integral

$$\int_{-\tau}^{\tau} x'_o(t) y_e(t)\, dt, \tag{5.28}$$

which contains, in the form of $x'_o(t)$, the time derivative of $\vec{v} \times \vec{E}/c^2$. For uniform electric field, this is proportional to the acceleration due to gravity and remains constant in free fall. With $x'_o(t)$ as a constant term, $\mathcal{B}^{(1)}_{2,2}$ is proportional to

$$\int_{-\tau}^{\tau} y_e(t)\, dt \;=\; \int_{-\tau}^{\tau} \beta_y(t)\, dt\ . \tag{5.29}$$

which is the integral of the vertical component of the magnetic field at each point along the trajectory between the atoms' entry into the electric field and their exit some 0.67 seconds later.

This is the same integral that can be measured directly by turning off the electric field, increasing slightly the launch velocity so that the location of the apogee of the trajectory is in the same place as it is when the electric field is on, and timing the vertical preparation and analysis laser pulses to occur as the atoms reach the point in space, as shown in Fig. 3.10, where the electric field steps occur when the electric field is on.

It is straightforward to turn on the current in a coil (Fig.'s 5.9, 5.13) to add whatever field is needed to make this *integral* nearly zero, without having to make β_y zero *at every point* along the atomic trajectory. The systematic $b_1 p_1$ displayed in Fig. 5.5 corresponds to a value of the integral in Eq. (5.29) of 174 fT s. The measurement of the field integral adapting our basic magnetometer (Sec. 3.9), with but four launches of 6.4×10^8 atoms of francium per launch, has a statistical sensitivity of 0.45 fT s; the counting time to tune the integral to make a negligible contribution to a measurement of an electron EDM at are target sensitivity will be a matter of minutes.

Cancellation by Polarization Rotation

The EDM signal (Fig. 5.5) has its maximum near $\pi/16$ at

$$\theta_1 = 0.2138 \tag{5.30}$$

and has a convenient node just past $3\pi/16$ at

$$\theta_2 = 0.6907\ ; \tag{5.31}$$

where the magnitude of the contribution from b_1 is large.

A true EDM signal vanishes at $\theta = 0.6907$.

Assuming that the contribution of b_2 is negligible, linear combinations that isolate the effect of an EDM and the remaining scalar are

$$\begin{aligned} D &= +\ \ 0.38314\,P(\theta_1) + 0.32385\,P(\theta_2) \\ b_1 &= -10.782\,P(\theta_1) + 0.48008\,P(\theta_2) \end{aligned} \tag{5.32}$$

Changing the angle θ of the linear polarization of the preparation laser is easily done by rotating an optical element or energizing a Pockels cell, so taking data at the two angles θ_1 and θ_2 is easily accomplished.

We have thus found a way to extract a value of D, and so of the electron EDM, in which any contribution from a finite value of b_1 cancels. A different linear combination of the same data extracts a value of b_1 that is independent of the presence of an electron EDM; we can therefore use the data to tune the magnitude of b_1 to be small[5].

This polarization angle dependence arises because different $|M|$ have different systematic and EDM sensitivities and changing the polarization angle θ changes the mix of $|5, \pm M\rangle$ states making up the superposition. This feature has some resemblance to a comagnetometer but is much better: it uses the same francium atoms, in the identical electric and magnetic fields, following identical trajectories. It can be used to reduce the b_1 systematic, be used as a diagnostic tool, and be used to distinguish a real EDM from a false EDM.

[5]With the cesium null EDM experiment (Section 7.3) using $M = 2$ we can make the $\mathcal{B}^1_{2,2}$ term 80 times larger (for the same static magnetic field) than for $F = 5$ in ^{211}Fr (See Appendix D). With the large Cs fountain intensity, the error b_1 and its dependence on θ can then be studied directly, with counting times of minutes rather than weeks.

5.3 Computation of $\mathbf{U_{rot}}$

Between the point of state preparation and the point where the atoms reach the step-function rise of the electric field, there will inevitably be stray magnetic fields; the approximation in Fig. 5.3, where the remnant magnetic field applied to the atom jumps discontinuously from zero at the instant an atom in the fountain crosses into the electric field, has to be repaired. Even with the discontinuous jump in the electric field, there will be fields between the point of state preparation and the point where the electric field jumps; the effect of such fields is to rotate the atomic state slightly, applying a unitary transformation

$$U_{\rm rot} = \exp\Big(-i(\alpha_x \mathbf{F}_x + \alpha_y \mathbf{F}_y + \alpha_z \mathbf{F}_z)\Big) \tag{5.33}$$

This is an exact result, however large and complicated the magnetic fields applied may be, and however large the resulting angles α may be. In practice we shall measure the angles α and apply extra fields using coils (see figures 5.14, 5.15) to tune the angles to be small, without however having to tune the total magnetic field everywhere to zero. Once the angles are small it will suffice to approximate

$$U_{\rm rot} \approx 1 - i\alpha_x \mathbf{F}_x - i\alpha_y \mathbf{F}_y - i\alpha_z \mathbf{F}_z\ . \tag{5.34}$$

Under the approximation of Eq. (5.5), we then have

$$U_{\rm net} \approx 1 - 2i\alpha_x \mathbf{F}_x - 2i\alpha_y \mathbf{F}_y - i2\alpha_z \mathbf{F}_z\ ; \tag{5.35}$$

distinguishing the effect of an electron EDM is easy, because though $U_{\rm net}$ does contain a small rotation about the z axis, the angle $2\alpha_z$ of that rotation is even in the applied electric field, while the rotation due to an electron EDM is odd.

The reversal of the electric field then separates this contribution from that of an EDM.

5.4 Motional Systematic Effects in the Electric Field Transition Region

5.4.1 Computation of U_{up} and U_{down}

The electric field cannot really have a step-function jump; it must increase from zero over some distance that is at least a small multiple of the separation between the electric field plates. An electric field profile achievable in a design that uses at the plate edge a set of electrostatic lenses (See Section 3.12) to focus the atomic beam is shown in Figure 5.6.

The corner on the lens has a relatively large radius to control the defocusing of atoms by gradients in the electric field [Kal11]. This field profile can be well approximated (Fig. 5.6) by a linear ramp, which for a practical plate half-gap of 6 mm extends over a distance of 3.95 cm.

We solve for the time evolution of the atom in the region of increasing field using the dimensionless Schrödinger equation and dimensionless Hamiltonian of Eqs. (5.9) and (5.10). In this section we use the symbol τ to denote the change in the dimensionless time variable t required for an atom to cross the region of increasing electric field (ramp); in practice the value of τ is $\sim 10^{-2}$, while the magnitudes of the components of the vector $\vec{\beta}$ are of rough order unity, so a series in powers of τ will converge rapidly. We will also ignore for the sake of simplicity the deceleration of the atom due to gravity and the acceleration of the neutral atom into the stronger electric field due to the atom's scaler polarizability (Fig. 3.23 and Section 3.12.1). These complicate but not change the essential conclusions of the analysis.

With these assumptions both the electric field and the motional magnetic field are, in the ramp region, linear functions of time; and we choose the zero of time to be such that $\int E^2\,dt$ over this region gives the same value as for a step-function rise over the same time-interval. The linear increase of the electric field over a total time τ is therefore as shown in Fig. 5.7.

We choose a fixed time interval $[-T, T]$, with T larger than any value of τ of interest, but still so

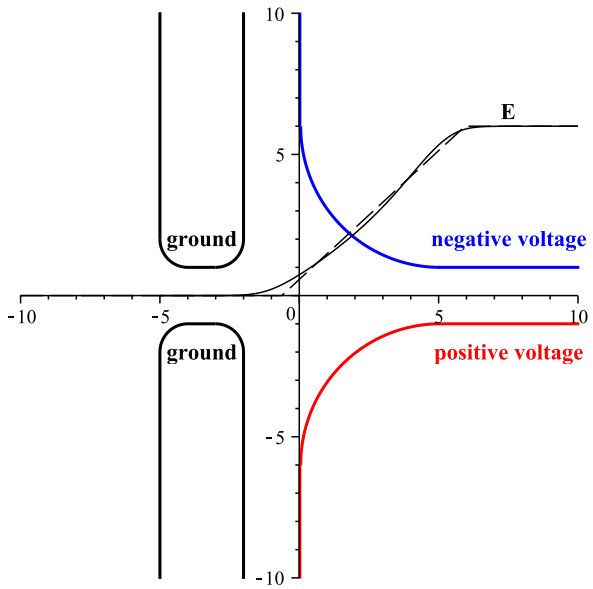

Figure 5.6: Design in cross section of a grounded aperture (C0 in Table 3.8 and Fig. 9.1) and the entrance to the D1 electrostatic lens. The distance scale is in units of 6 mm, which is half the gap between electrostatic lens plates at the center axis. The profile of the electric field is shown as the solid black curve; the grounded aperture creates a faster decrease of the electric field to zero. Also shown (dashed line in black) is the best approximation of the actual field profile by a simple linear ramp.

small that for any times t_1 and t_2 in that interval, and for any Hamiltonian H of interest, the Freeman-Dyson series

$$U(H;t_1,t_2) = 1+(-i)\int_{t_1}^{t_2} H(t)\,dt + (-i)^2\int_{t_1}^{t_2}\int_{t_1}^{t} H(t)H(t')\,dt'\,dt + \cdots \tag{5.36}$$

that gives the time evolution is rapidly convergent. The time evolution in the presence of the ramp is

$$U_{\rm ramp} = U(H_{\rm ramp};-T,T)\ , \tag{5.37}$$

where for the Hamiltonian $H_{\rm ramp}$ we have for the

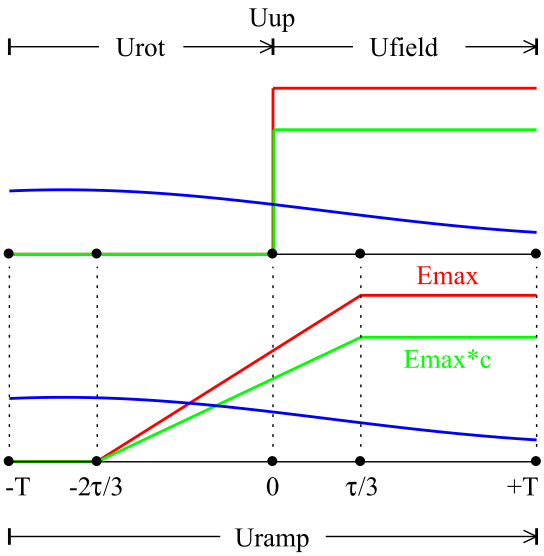

Figure 5.7: For a beam of constant velocity c, the lower half of this figure shows in red a linear ramp of the electric field applied to an atom rising from 0 to $E_{\max}$ over a time τ, in green the corresponding linear ramp of the motional magnetic field, and in blue the magnetic field applied to the atom due to its motion through a supposed spatially-varying static magnetic field. The upper half shows the corresponding fields when the electric field is modeled to have a step-function jump; the location of the jump is chosen so that $\int_{-T}^{T} E_z^2(t)\,dt$ is the same for the ramp and for the jump. The unitary transformation U_{ramp} due to the actual linear ramp is equated to the product of a simple rotation U_{rot} in zero electric field; a correction term U_{up} we seek to determine, and the evolution U_{field} in when both the electric and motional magnetic fields are constant.

electric field $\epsilon_z(t)$ just

$$\begin{cases} 0 & \text{for } t < -2\tau/3 \\ \epsilon^2 t^2/\tau^2 + \frac{4}{3}\epsilon^2 t/\tau + \frac{4}{9}\epsilon^2 & \text{for } -2\tau/3 < t < \tau/3 \\ \epsilon & \text{for } -\tau/3 < t\ , \end{cases} \tag{5.38}$$

with the magnetic fields

$$\begin{aligned} \beta_x(t) &= c\epsilon_z(t) + x_0 + x_1 t + x_2 t^2/2 + \cdots \\ \beta_y(t) &= y_0 + y_1 t + y_2 t^2/2 + \cdots \\ \beta_z(t) &= z_0 + z_1 t + z_2 t^2/2 + \cdots\ , \end{aligned} \tag{5.39}$$

where c is the atomic velocity, and where we have approximated the static magnetic fields by the first terms in their Taylor series. When the electric field makes a step-function jump at time zero, the unitary transformation that applies to the atom before the jump is

$$U_{\text{rot}} = U(H_{\text{rot}}; -T, 0)\ , \tag{5.40}$$

where for the Hamiltonian H_{rot} we have the fields when the electric field is zero, which are

$$\begin{aligned} \epsilon_z(t) &= 0 \\ \beta_x(t) &= x_0 + x_1 t + x_2 t^2/2 + \cdots \\ \beta_y(t) &= y_0 + y_1 t + y_2 t^2/2 + \cdots \\ \beta_z(t) &= z_0 + z_1 t + z_2 t^2/2 + \cdots\ . \end{aligned} \tag{5.41}$$

After the jump, the unitary transformation that applies is

$$U_{\text{field}} = U(H_{\text{field}}; 0, T)\ , \tag{5.42}$$

where for the Hamiltonian H_{field} we have the fields when the electric field is constant,

$$\begin{aligned} \epsilon_z(t) &= \epsilon \\ \beta_x(t) &= c\epsilon + x_0 + x_1 t + x_2 t^2/2 + \cdots \\ \beta_y(t) &= y_0 + y_1 t + y_2 t^2/2 + \cdots \\ \beta_z(t) &= z_0 + z_1 t + z_2 t^2/2 + \cdots \end{aligned} \tag{5.43}$$

We define a unitary transformation U_{ramp} for an upward sloping ramp of the electric field by

$$U_{\text{ramp}} = U_{\text{field}} U_{\text{up}} U_{\text{rot}}\ , \tag{5.44}$$

where in the limit $\tau \to 0$ we have $U_{\text{up}} = 1$; solving, we have

$$U_{\text{up}} = U_{\text{rot}}^\dagger U_{\text{ramp}} U_{\text{field}}^\dagger\ . \tag{5.45}$$

Thus the transformation U_{up}, that allows us to compute the total unitary transformation U_{net} from state preparation through state analysis, is just the product in Eq. (5.3). The three transformations on the right can all be computed as convergent series in τ, and so therefore can U_{up}. With a velocity through the ramp-up region[6] of 4.02 m/s, the time to cross the ramp is $9.81 \cdot 10^{-3}$ s; the corresponding dimensionless time used to expand the Freeman-Dyson series is $\tau = 1.12 \cdot 10^{-2}$. Because the typical values of the fields involved are in a practical fountain of rough order unity, the series in τ converges quickly.

[6] This velocity is now closer to 3.0 m/s but this change has no significant effect on the result.

The resulting series for the correction for the atom entering the field is

$$U_{\rm up} = \Big(1 - \frac{iQ\tau}{6} - \frac{Q^2\tau^2}{72}\Big) + \Big(\frac{1}{18}[Q,P] + \frac{1}{90}[R,Q] + \frac{1}{36}[R,P]\Big)\tau^2 + O(\tau^3)\ . \tag{5.46}$$

Here we have

$$\begin{aligned} P &= x_0\mathbf{F}_x + y_0\mathbf{F}_y + z_0\mathbf{F}_z \\ Q &= c\epsilon\mathbf{F}_x \\ R &= \epsilon^2\mathbf{F}_z^2 \end{aligned} \tag{5.47}$$

The first line of Eq. (5.46) contains a rotation about the x direction by an angle

$$\xi = c\epsilon\tau/6\ , \tag{5.48}$$

since we recognize the first terms in the expansion of a rotation operator,

$$\exp(-i\xi\mathbf{F}_x) = \Big(1 - \frac{iQ\tau}{6} - \frac{Q^2\tau^2}{72}\Big) + O(\tau^3)\ . \tag{5.49}$$

Such a rotation as part of $U_{\rm up}$ is expected. The tensor Stark effect is quadratic in the electric field, while the motional magnetic field is but linear; as the electric field limits to zero at points further and further from the entrance to the electric field plates, there has to be a region where the motional magnetic field is still appreciable and the tensor Stark effect is negligible. There has then to be a small rotation about the motional magnetic field that isn't accounted for in the approximation where the electric field jumps discontinuously from zero, whereas in the approximation of an electric field jump, there is no motional magnetic field in any region where tensor Stark effect is negligible.

The angle ξ of this rotation (see Eq. (5.48)) is linear in ϵ and so, like the rotation effected by an EDM, this rotation is odd in the electric field. The two rotations can be distinguished because the axes about which they occur are perpendicular; the motional magnetic field arises from the cross product in the Lorentz transform

$$\vec{B} = \frac{1}{c^2}\vec{v}\times\vec{E} \tag{5.50}$$

where $\vec{v}$ is the particle velocity[7] and $\vec{E}$ is the electric field vector; the rotation due to an electron EDM occurs about $\vec{E}$, and the rotation due to the motional magnetic field occurs about $\vec{B}$. However the danger in the ξ-rotation is that it can combine with rotations about the y axis due to static magnetic fields and generate a net field-odd rotation about the z axis.

While it would be desirable therefore to make the angle ξ small, doing so comes at a price. The angle ξ depends on the product $c\tau$, which is the distance over which the field ramps up. That distance is set in part by the separation of the D1 electrodes; the curvature of the electrode ends; and the distance to C0, the electric field ground clamp (Fig. 5.6). The values for all of these have been chosen to maximize transmission of atoms through the electric field.

The angle ξ is independent of the atomic velocity; while we have computed this to be true in the approximation that the atomic velocity is constant, and while atoms accelerate appreciably as they enter the electric field, a more refined analysis shows that the angle ξ is independent of how the velocity changes as the atom enters the electric field; it would remain the same if we could reach in with tweezers and make the atoms velocity change in an arbitrary manner provided only the atom started outside the electric field and ended within it.

The angle ξ depends only on the path the atom takes as it enters the field, not on how fast or how slow it traverses that path; it is the first occurrence in our analysis of a strictly path-dependent and velocity-independent, or "geometric," effect.

There is no special difficulty with extending the computation of $U_{\rm up}$ to higher order, though as a practical matter one has to use a computer algebra program such as Maple$^{\rm TM}$, instead of paper and pen, to get the results. The series for $U_{\rm up}$ has 54 terms of order τ^3, which are listed in the Appendix in Eq. (B.5).

The unitary transformation $U_{\rm down}$, that describes transformation for a ramp in the electric field down

[7] In Eq. (5.50) the variable c is the speed of light and not the particle velocity.

instead of up, can be obtained from $U_{\rm up}$ by an argument based on time symmetry. If electric and magnetic fields when applied to an atom generate a transformation U, then if time is reversed the electric field is applied in the reverse time order, and the magnetic fields are applied in the reverse time order and with a global change in sign; and the transformation generated must be $U^{-1} = U^\dagger$.

When an atom in a strict fountain falls out of the electric field plates, the electric field is applied in reverse time order with no change in sign; the motional magnetic field is applied in reverse time order with a global change in sign; but while the magnetic fields due to the atom's motion through laboratory static magnetic fields are applied in reverse time order, they are applied with no change in global sign. Therefore $U_{\rm down}$ follows by taking the Hermitian conjugate of $U_{\rm up}$ and changing the global sign of all the static magnetic fields. This prescription applied to Eq. (5.46) produces for example

$$\begin{aligned} U_{\rm down} =& \Big(1 + \frac{iQ\tau}{6} - \frac{Q^2\tau^2}{72}\Big) \\ &+ \Big(\frac{1}{18}[Q,P] - \frac{1}{90}[R,Q] + \frac{1}{36}[R,P]\Big)\tau^2 \\ &+ O(\tau^3)\ . \end{aligned} \tag{5.51}$$

The rotation about the motional magnetic field axis reverses direction.

5.4.2 Systematics Effects from $\mathbf{U_{up}}$ and $\mathbf{U_{down}}$

We now examine some systematic errors that result. If we zero by hand the angles α in the formula of Eq. (5.3) for $U_{\rm rot}$, and zero by hand all terms of order $1/\mu$ in $U_{\rm field}$ and assume $k_\epsilon + k_\beta = 1$, then from Eq. (5.3) we find that the unitary rotation applied to an atom would be

$$U_{\rm net} \to U_{\rm up} U_{\rm down}\ . \tag{5.52}$$

The product $U_{\rm up}U_{\rm down}$ is somewhat easier to manage than either term separately because $U_{\rm up}$ and $U_{\rm down}$ are intimately related by time-reversal and so there are a lot of cancellations in the product. Adopting the simplified notation

$$X = \mathbf{F}_x\ , \qquad Y = \mathbf{F}_y\ , \qquad \text{and} \quad Z = \mathbf{F}_z\ , \tag{5.53}$$

we find $U_{\rm down}U_{\rm up}$ equals $1 + O(\tau^4)$ plus the corrections

$$\begin{array}{lllll}
-1/18 & & \epsilon^2\, y_0 & [Y,ZZ] & \tau^2 \\
-1/18 & & \epsilon^2\, x_0 & [X,ZZ] & \tau^2 \\
+1/9 & c\ \epsilon & y_0 & [X,Y] & \tau^2 \\
+1/9 & c\ \epsilon & z_0 & [X,Z] & \tau^2 \\
+4/405 & ic^2\epsilon^2 & y_0 & \{XX,Y\} & \tau^3 \\
-8/405 & ic^2\epsilon^2 & y_0 & XYX & \tau^3 \\
+4/405 & ic^2\epsilon^2 & z_0 & \{XX,Z\} & \tau^3 \\
-8/405 & ic^2\epsilon^2 & z_0 & XZX & \tau^3 \\
+1/405 & & \epsilon^2\, x_1 & [X,ZZ] & \tau^3 \\
+1/405 & & \epsilon^2\, y_1 & [Y,ZZ] & \tau^3 \\
+2/567 & i & \epsilon^4\, x_0 & \{X,ZZZZ\} & \tau^3 \\
-4/567 & i & \epsilon^4\, x_0 & ZZXZZ & \tau^3 \\
+2/567 & i & \epsilon^4\, y_0 & \{Y,ZZZZ\} & \tau^3 \\
-4/567 & i & \epsilon^4\, y_0 & ZZYZZ & \tau^3 \\
-5/324 & c\ \epsilon & y_1 & [X,Y] & \tau^3 \\
-5/324 & c\ \epsilon & z_1 & [X,Z] & \tau^3 \\
-4/405 & ic\ \epsilon^3 & x_0 & \{XX,ZZ\} & \tau^3 \\
+8/405 & ic\ \epsilon^3 & x_0 & XZZX & \tau^3 \\
+4/405 & ic\ \epsilon^3 & y_0 & (XZZY + YZZX) & \tau^3 \\
-1/81 & ic\ \epsilon^3 & y_0 & (XYZZ + ZZYX) & \tau^3 \\
+1/405 & ic\ \epsilon^3 & y_0 & (YXZZ + ZZXY) & \tau^3 \\
-1/405 & ic\ \epsilon^3 & z_0 & \{X,ZZZ\} & \tau^3 \\
+1/405 & ic\ \epsilon^3 & z_0 & (ZXZZ + ZZXZ) & \tau^3\ ,
\end{array} \tag{5.54}$$

where $[\cdots]$ and $\{\cdots\}$ represent respectively commutators and anticommutators. The terms have been grouped into terms of order τ^2 that are even in the electric field; those of order τ^2 that are odd; those of order τ^3 that are even; and those of order τ^3 that are odd. Any terms that can mimic an EDM have to be odd in the electric field. The most dangerous of these terms are those in lines 3 and 15 of Eq. (5.54), which are

$$\begin{aligned} &\Big(\frac{1}{9}\, y_0 - \frac{5}{324}\, y_1\tau\Big) c\epsilon\tau^2 [\mathbf{F}_x, \mathbf{F}_y] \\ &= \Big(\frac{1}{9}\, y_0 - \frac{5}{324}\, y_1\tau\Big) c\epsilon\tau^2 i\mathbf{F}_z\ . \end{aligned} \tag{5.55}$$

As expected from qualitative arguments about the products of rotations, the vertical component y_0 of

the remnant magnetic field in the ramp-up region has interacted with the motional magnetic field in the ramp-up region to generate a net rotation about the electric field (z) axis that is odd in the electric field. The gradient in the vertical component of the remnant magnetic field (which is proportional to y_1) generates a correction that appears at higher order in τ.

Both this contribution and the contribution of an electron EDM to $U_{\rm net}$ are proportional to the operator $i\mathbf{F}_z$, so both represent rotations by a small angle about the z axis; and both rotations are odd in the electric field. This contribution therefore represents an electric-field odd EDM mimic whose leading term, in this model, is linear in the electric field.

In a practical apparatus with an initial stray magnetic field in the vertical direction of 163 fT, the net rotation angle has a magnitude of $2.5 \cdot 10^{-7}$ rad, which is essentially the same as the rotation angle due to an electron EDM of 1.3×10^{-50} C m. To detect such an e-EDM we require y_0, and by extension the vertical component of the magnetic field throughout the ramp-up region, to have a magnitude of < 163 fT.

A magnetic field of < 163 fT is well within our goal of magnetic fields of ≤ 20 fT and close to our initial goal of magnetic fields ≤ 200 fT. Significantly, this vertical component of magnetic field (with not too large a gradient, see Eq. 5.55) is required only within the ≈ 4 cm transition region. Magnetic field nulling coils to reduce the vertical component of magnetic field and the magnetic field gradient specifically in the transition region have been designed and are shown in Figs. 5.11 and 5.12. These coils will be tested in the magnetic prototype fountain (Section 7.1) and the effect of magnetic fields in the transition region will be studied using the cesium fountain EDM null apparatus (Section 7.3).

Should it prove necessary, the transition region may be made smaller, first by decreasing the 2.4 cm distance between C0 and D1 and then by reducing the radius of curvature of the bottom end of D1. Reducing the transition region by a factor of two will raise the allowed vertical magnetic field by a factor of four.

5.5 Reducing Magnetic Fields to fT levels

5.5.1 Magnetic Shielding Requirements

The four-layer magnetic shielding for the EDM experiment has a calculated axial (vertical) shielding factor of 1.6×10^6 (Table 8.2). It will reduce the ambient magnetic field at TRIUMF ISAC (Fig. 4.5) of 1.4×10^{-5} T to below 10 pT and the axial magnetic noise (Fig. 4.5) of $\pm 3.3 \times 10^{-8}$ T to about ± 200 fT. An additional external solenoid coil with magnetometer and control circuit (active shield, see Section 8.3) can reduce the residual magnetic field[8] and the magnetic noise by another factor of 10 to 100, resulting in a residual magnetic field of 100 fT to 1000 fT and axial magnetic noise of 2 fT to 20 fT. (If there were no other sources of static magnetic fields, residual magnetic fields of 100 fT would be sufficiently small to allow systematic sensitivity of below 1×10^{-50} C m without needing coils inside the shielding to null the residual magnetic fields.)

As the mu-metal shields are ferromagnetic, the inner shield (S5 in Fig. 3.2) will, unless demagnetized, produce a massive magnetic field. Demagnetization is commonly done using alternating currents (A.C. demagnetization, see Section 8.5) but can also be done by heating above the Curie point as is done on geological samples in paleomagnetism studies. Because the Curie point for mu-metal is around 460 °C, and the presumed resulting fields are too small to be measured by all but the most sensitive absolute field measuring magnetometers, we know of no experimenter who has as yet investigated thermally demagnetized mu-metal.

Results of A.C. demagnetization on three nested magnetic shields, from our prototype shield set, are shown in Fig. 8.7. Remnant magnetic fields of up

[8] In principle all that is needed is to statically null the axial component of the ambient field, neglecting the small variations. However a full active system protects against movement of the overhead crane, and other field altering events.

to 200 pT in the radial directions are seen and these vary despite seemingly identical demagnetizations. The remnant field in the axial direction at the center of the shield is about 50 pT and changes only slowly with axial position. The axial fields also vary from one demagnetization to the next, but about one in five demagnetizations produces an axial field profile with the fields ≤ 50 pT and the small gradients seen in Fig. 8.7. The measured magnetic field in the axial direction may have a component from a room magnetic field gradient not entirely shielded by the three layer axial shielding factor of 2.9×10^5.

The Magson digital fluxgate magnetometer used for these measurements has uncertainties of several tens of pT (exceptionally good for a fluxgate magnetometer but still thousands of times noisier than the francium fountain), limiting the scale of demagnetizing experiments that could be undertaken. Once a cesium fountain apparatus is available for magnetometry (Section 7.1) far more sensitive demagnetization experiments, including some using thermal demagnetization, will be done.

5.5.2 Magnetic Field Nulling

The most important systematic terms are dependent on the axial magnetic field. Using the measured 50 pT axial field as a starting point, we can, subject to the constraints of our present magnetometer and existing shields and A.C. demagnetizing technique, examine how far magnetic fields can already be lowered in the sensitive regions of the experiment. If the field is steady and uniform there is almost no limit to how well it can be nulled. We know that it is steady but not especially uniform.

An unsteady field will show up as noise. Several investigators with magnetometers very sensitive to magnetic noise, but not necessarily able to measure small absolute magnetic fields, have investigated the magnetic noise inside of shields at the fT level. Thiel et al. [TSS+07b] measured magnetic field noise inside a magnetically shielded room and found noise of $5\,\mathrm{fT}/\sqrt{\mathrm{Hz}}$ at 1 Hz with $\geq 15\,\mathrm{fT}/\sqrt{\mathrm{Hz}}$ spikes between 6 Hz and 8 Hz due to vibration of the magnetometer in the magnetic field gradient. Kornack et al. [KSLR07] measured magnetic field noise inside a ferrite shield surrounded by nested mu-metal shields and found about $15\,\mathrm{fT}/\sqrt{\mathrm{Hz}}$ of noise at 0.5 Hz. We repeated a measurement of the remnant magnetic fields inside our test shields (Fig. 8.7) after four days. The average change of ≈ 10 pT(well within the magnetometer uncertainty) over 96 hours sets a limit to the drift in the field of about 100 fT/hour. The magnetic prototype fountain (Section 7.1) will allow us to make measurements a hundred times more sensitive.

The magnetic field gradients pose more of a problem when a low magnetic field component is needed in a specific region such as the transition region (Section 5.4.2), rather than when setting the integral of a component of magnetic field over the beam trajectory (Section 5.2.2). For the 4 cm transition region to have a field of magnitude 163 fT over its entire length, the magnitude of the magnetic field gradient needs to be ≤ 136 fT/cm. That may presently be met with no gradient nulling coils in the very center of the test shield (Fig. 8.7), but outside of that region, the magnetic field gradient grows to 2.3 pT/cm and higher towards the ends. Thus, absent improvements in demagnetizing technique, one or more gradient coils will also be needed. (If the transition region is reduced to 2 cm, the magnetic field can rise to 652 fT and the gradient to ≤ 1.09 pT/cm.) In what follows, we show designs for magnetic field nulling coils and magnetic field gradient nulling coils.

If thermal demagnetization is successful, the field inside the inner shield would be the result of remnant magnetic field from the next outer shield, attenuated by the shielding factor of the inner shield. The axial shielding factor of S5 is calculated to be about 85, so a 100 pT remnant field in S6 would be reduced to about 1 pT inside S5. We would also expect only a small magnetic field gradient.

5.5.3 Magnetic Field Nulling Coil Design

Sets of magnetic field coils will be used to null the

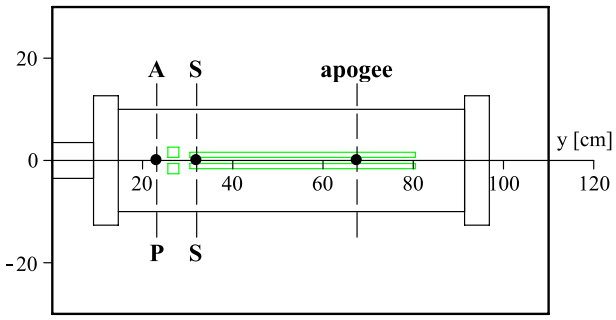

Figure 5.8: Schematic of an atomic fountain apparatus; for convenience, the apparatus is shown with what will be the vertical, y, axis shown horizontally on the page. Dimensions are in cm. The heavy black outer rectangle indicates the inside surface of the innermost cylindrical magnetic shield (not to scale). The thin black lines indicate the perimeter of the vacuum vessel. The clamp-field plates (C0) held at zero potential are indicated in cross section by the small green squares; the main electric field plates (including the electrostatic lenses) are indicated in cross section by the longer thin rectangles in green. Atoms enter the apparatus at the left, slow to zero velocity at the point indicated by "apogee" and turn around and exit to the left. The dashed line at the far left indicates the location of the point P of state preparation region, which is the same point A at which analysis occurs as the atoms exit. The atoms experience an effective jump from zero to full electric field at the point S.

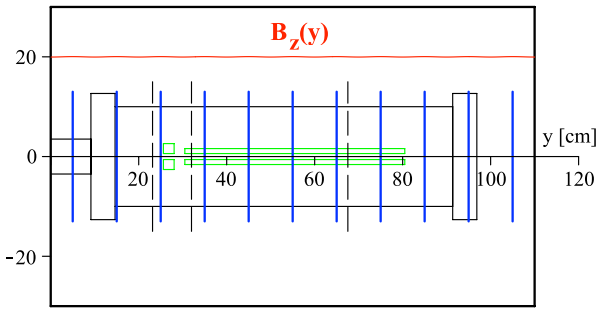

Figure 5.9: Axial magnetic field coils: overlaid on the schematic of Fig. 5.8 is a regular array of 11 circular coils, indicated in blue. The coils are outside the vacuum system. Plotting in red is the resulting essentially constant component of the component of the resulting magnetic field along the y direction at points on the y axis.

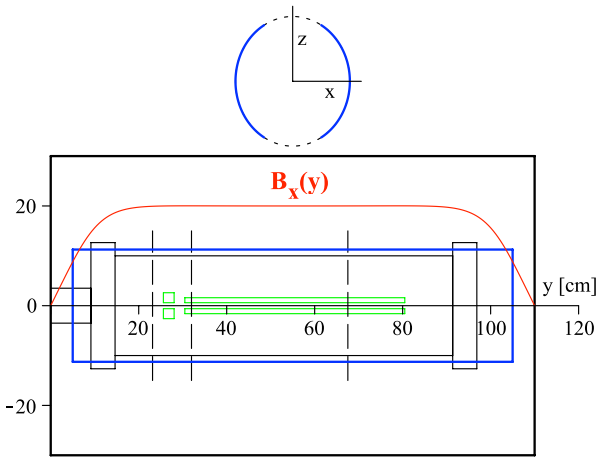

Figure 5.10: Transverse magnetic field coils: overlaid on the schematic of Fig. 5.8 is a pair of coils, indicated in blue; as is indicated in the upper part of the figure, the wires of these coils are confined to a cylindrical surface. The coils are outside the vacuum system. Plotted in red is the resulting magnetic field along the x direction at points on the y axis.

vertical magnetic field and magnetic field gradient in the transition region, and just inside the electric field, and at the fountain apogee. Other coils will be used to null the magnetic fields in the transverse directions. Fig. 5.8 shows a schematic of the interaction region with the locations of state preparation and analysis, the grounded electric field clamp, and the electric field plate assembly with its electrostatic focusing triplet. The effect of the the surrounding cylindrical magnetic shield has been included in the computations that follow of the fields generated by various coils.

Extended magnetic fields

We consider first generating fields in three directions over the length of the interaction region. A schematic of the fountain is shown in Fig. 5.8. Overlaid on that schematic in Fig. 5.9 is a an array of 11 circular coils; along the y axis the resulting axial field in the y direction is uniform to 0.4%.

Also overlaid on that schematic in Fig. 5.10 are a pair of coils for generating a magnetic field in the x direction whose wires fit on a cylindrical surface. The boundary condition for the magnetic field forces this component of the magnetic field to vanish

at the flat faces (end caps) of the magnetic shield; nonetheless along the y axis the resulting field in the x direction is, starting at the point of state preparation, uniform to 0.3%.

A second pair of coils rotated about the y axis by $\pi/2$ will generate a corresponding field in the z direction.

Local axial magnetic fields and gradients

A pair of coils in a near Helmholtz configuration, shown in Fig. 5.11, provides magnetic field in the y direction at the point where the electric field effectively jumps from zero. With these coils we can adjust the value of the vertical component of the magnetic field $y_e(-\tau)$, or the vertical gradient of this component.

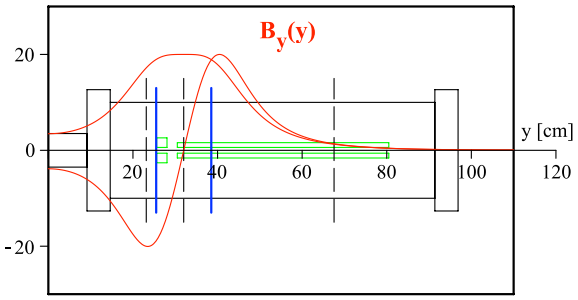

Figure 5.11: Axial magnetic field and gradient coils near electric field entrance: Overlaid on the schematic of Fig. 5.8 is a pair of circular coils, indicated in blue. Plotted in red is the resulting magnetic field along the y direction at points on the y axis, when the coils are energized in a Helmholtz and in an anti-Helmholtz configuration, providing a respectively a constant field and a uniform gradient at the point where the electric field makes its effective jump from zero.

Adding a third coil, as shown in Fig 5.12, allows the adjustment of the time integral of the magnetic field between the point of state preparation and the point where the electric field effectively jumps from zero, without changing either the value of the field at that point or its gradient. This configuration allows a tune of α_y. Finally to tune the last systematic b_2 to be of small magnitude, it is desirable to be

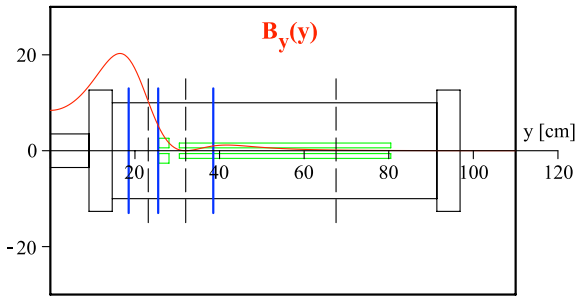

Figure 5.12: Axial magnetic field and gradient coils for the transition region: Added to Fig. 5.11 is a third circular coil. Plotted in red is an achievable magnetic field along the y direction at points on the y axis, when the coils are given appropriate currents. The value and the gradient of the field are zero at the point where the electric field makes its effective jump from zero.

able to change the time integral of B_y with minimal disturbance of either $y_e(-\tau)$ or of α_y.

Because the atom spends most of its time near apogee, this can be effected by adjusting a single current loop located near apogee; little field from this loop appears at the entrance to the electric field plates, and the atom spends little time in that region. The loop and the resulting field is shown in Fig. 5.13.

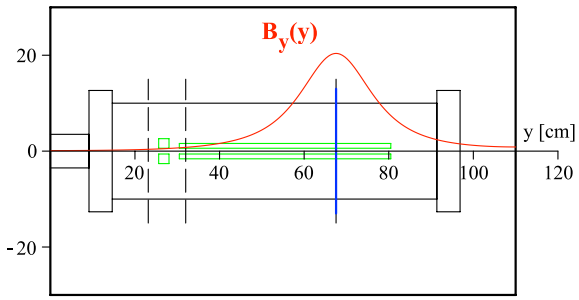

Figure 5.13: Axial magnetic field coil for the apogee: Overlaid on the schematic of Fig. 5.8 is a circular coil, indicated in blue at the location of the apogee of the atoms. Plotted in red is the resulting magnetic field along the y direction at points on the y axis.

Local transverse magnetic fields and gradients

Coils for the fields we need in the x direction are similar. Shown in Fig. 5.14 are two pairs of coils in an almost-Helmholtz configuration, which can provide any combination of a constant or a constant-gradient field in the x direction at the point where the electric field makes its effective jump. Such coils allow tuning of $x_e(-\tau)$ or if necessary its derivative. Adding a third such pair, as shown in Fig. 5.15, gives the flexibility to change the time integral of B_x between the point of state preparation and the point where the electric field makes its effective jump from zero, and so to change the value of α_x, without also changing either $x_e(-\tau)$ or its gradient.

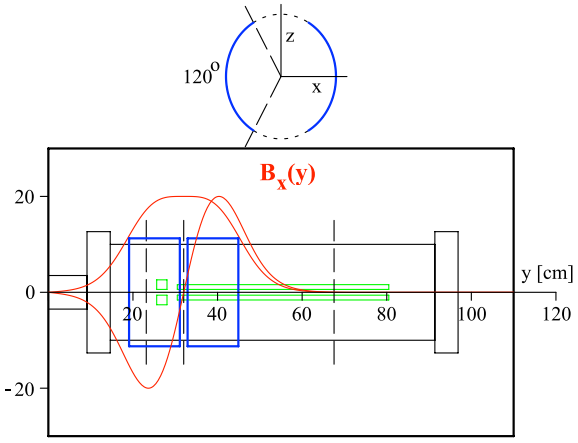

Figure 5.14: Transverse magnetic field and gradient coils for electric field entrance: In blue, are two pairs of coils. All the wires of the coils are confined to the surface of a cylinder. Plotted in red is the resulting magnetic field along the x direction at points on the y axis, when the coils are energized in a Helmholtz and in an anti-Helmholtz configuration, providing a respectively a constant field and a uniform gradient at the point where the electric field makes its effective jump from zero.

A set of coils identical except for being rotated about the vertical axis by $\pi/2$ allows for tuning of $z_e(-\tau)$ or if necessary its derivative, or the flexibility to change the time integral of B_z between the point of state preparation and the point where the electric field makes its effective jump from zero, and so allows for the tuning of α_z.

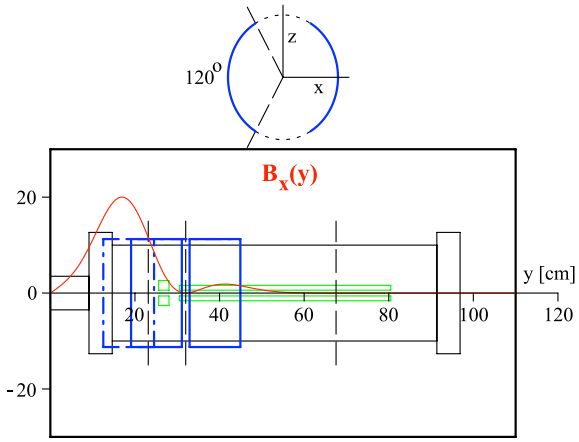

Figure 5.15: Transverse magnetic field and gradient coils. Added to the coils in Fig. 5.14 is a third coil, shown in blue dash-dot. Plotted in red is an achievable magnetic field along the x direction at points on the y axis, when the coils are given appropriate currents. The value and the gradient of the field are zero at the point where the electric field makes its effective jump from zero.

5.6 Tuning the Atomic Fountain

The parameters and fields that are necessary to be tuned to zero or near zero are:

1. Stray magnetic fields between the point of state preparation and the entrance to the electric field plates: these may rotate the atomic state by angles α_x and α_y about the x and y axes, respectively, before the atoms enter the electric field.

2. An incremental departure a of the Stark phase from an integer multiple k_ϵ of π, namely

$$\int_{-\infty}^{\infty} \epsilon_z^2(t)\, dt - k_\epsilon \pi = a \ . \tag{5.56}$$

3. An incremental departure b of the Zeeman phase advance between state preparation and state analysis from an integer multiple k_β of π (we recall we will set $k_\beta = 0$) , namely

$$\int_{\text{preparation}}^{\text{analysis}} \beta_z(t)\, dt - k_\beta \pi = b \ . \tag{5.57}$$

4. Magnetic fields between the point of state preparation and the point in space where the

electric field makes its effective discontinuous step. They rotate the state by an angle α_z about the z axis, there being a compensating rotation by $-\alpha_z$ from the point the atoms enter the electric field plates to where the atoms reach apogee, so that

$$\int_{\text{preparation}}^{\text{step}} \beta_z(t)\, dt = \alpha_z \ . \tag{5.58}$$

This is a problem even if the Zeeman phase accrued from state preparation all the way to state analysis has been locked to zero,

5. Magnetic fields in the x, y, and z directions with components x_e, y_e, and z_e at the entrance to the electric field plates and with possible vertical gradients in each of these (even if all angles and phases in (3) and (4) above, which all depend on time integrals over magnetic fields, were zero).

First we use the coils described in Fig. 5.9 and Fig. 5.10 to separately null, in x, y, and z, the integral of the magnetic field between state preparation and analysis.

Our next step is to turn on the electric fields and tune the Stark phase in (2) to a multiple of π.

We next superimpose on the remaining magnetic fields such additional magnetic fields as will tune the systematics in an electron EDM measurement to zero, without having to null or even measure everywhere the remnant magnetic field.

To accomplish this tune requires three laser beams that have a common intercept at the common point of state preparation and analysis below the electric field plates. One laser propagates vertically, in the y direction; and two propagate horizontally, one perpendicular to the electric field plates, in the z direction; and one parallel to the electric field planes, in the x direction. Each laser has a counter propagating laser beam to eliminate any net gain of momentum by the atomic beam as a result of optical pumping.

Parameters which are small but which we cannot adjust to zero result in the remaining sensitivity to systematics. These parameters are

- The ratio of the size of the Zeeman splitting due to typical ambient magnetic fields to the Stark splitting. This is $\sim 3\times10^{-5}$ for a 200 fT magnetic field and $\sim 3\times10^{-3}$ for a 20 pT field.
- The time ratio of the atoms spend in the transition region where they see the electric field ramp from zero to its full constant value to the total time the atoms spend in the apparatus; this ratio is $\sim 1\times10^{-2}$.

We will classify magnitudes as $O(n)$ if the magnitude has a total power of n in these two small parameters. Initially all parameters have a magnitude of order unity, or $O(0)$ in the small parameters; we do a sequence of measurements[9] that gradually reduce the critical parameters so that the error in an electron EDM experiment, computed using the full unitary transformation between state preparation and state analysis, will give an error in the electron EDM of O(3) in the small parameters.

With 200 fT fields, only terms in the ratio of Zeeman to Stark splitting of O(1) or, at most, O(2) will be needed. However for completeness we carry the calculation out to higher order.

The flexibility to find a sequence of measurements comes not only from the freedom to select the direction of the preparation and analysis lasers but to select their polarization and frequency. While one set of probabilities c_M of remaining in the upper hyperfine level when starting in a state $\left|5M\right\rangle$ has been presented in Fig. 3.7, eleven others are also available, as shown in Appendix B.5 and Figure B.1. The steps in the simplest sequence worked out so far, run as follows:

[9] In finding this sequence intuition plays little role; it is akin to exploring a large but finite maze and finally getting a prescription for getting from point A to point B.

The initial tune uses four independent measurements to reduce four parameters in magnitude from $O(0)$ to $O(1)$. The specific information about the lasers and polarizations required is encoded in the following table:

(a)	(b)	(c)	(d)	(e)	(f)	(g)	(h)	(i)	(j)	(k)	(l)
α_x	x	Π	z	0	x	Π	z	θ	θ_-	k even	$\lvert\theta\rvert = 0.21209$
α_y	y	Π	z	0	y	Π	z	θ	θ_-	k even	$\lvert\theta\rvert = 0.21209$
a	x	Π	z	θ	x	Σ	$\ldots$	$\ldots$	$\theta_-\Sigma_-$	$\ldots$	$\lvert\theta\rvert = \pi/4$
b	z	Π	x	θ	z	Π	x	0	θ_-	$\ldots$	$\lvert\theta\rvert = 0.21209$

(5.59)

One reads the third line, for example, left to right as, "To see the shift a of the tensor Stark phase[10], prepare the atoms with a laser that propagates parallel to the x axis, that is linearly (Π) polarized with its axis of linear polarization making with respect to the z axis an angle equal to θ. Analyze the atoms with a laser that propagates parallel to the x axis and that is circularly (Σ) polarized. To isolate the shift, combine data chopping polarization angle and subtracting (θ_-) and chopping in helicity and subtracting (Σ_-); there is no requirement for the integer k to be even or odd; and for optimum results the magnitude of the polarization angle must be set ($|\theta| = \pi/4$)."

In general the significance of the various columns is

(a) parameter that is zero when the observable is zero
(b) axis of preparation laser propagation
(c) laser polarization (linear is Π, circular is Σ)
(d) if linear, axis with respect to which the angle of linear polarization is measured
(e) if linear, angle to which the linear polarization is to be set
(f) axis of analysis laser propagation
(g) laser polarization (linear is Π, circular is Σ)
(h) if linear, axis with respect to which the angle of linear polarization is measured
(i) if linear, angle to which the linear polarization is to be set
(j) which parameters alternate and whether one adds ($+$) or subtracts ($-$) in forming the observable
(k) whether the parameter $k = k_\epsilon + k_\beta$ has to be even or odd
(l) settings that maximize sensitivity

(5.60)

The tunes of α_x, α_y, and of b use the magnetometers of Figures 3.10, and 3.11, respectively, with an analysis angle θ whose magnitude maximizes sensitivity. The tune of a, the departure of the tensor Stark phase from $k_\epsilon\pi$, is new; and is the first tune that uses (for analysis) circularly polarized light[11].

In the unitary operator U_{field}, which describes the region of constant electric field, six parameters $\mathcal{G}$ and $\mathcal{B}$ occur at order $1/\mu$; these allow extraction of information about the static magnetic fields within the constant field region and (critically) at the point where the electric field makes its effective jump. These six parameters unfortunately go by several different notations with different schemes of indices; a table of the notation used in this paper, and that in Ref. [WMJ12], follows. Formulas for the parameters themselves may be found in the Appendix in Eqs. (B.9)–(B.14).

[10] From $k_\epsilon\pi$, see Eq. (3.51) or Eq. (5.56)

[11] We do not idly introduce the complication of using circularly polarized light; sadly, it has been proven that all systems that use linearly polarized light for both state preparation and state analysis yield observables that depend quadratically instead of linearly on a, and so yield inefficient signals for $|a| \ll 1$. Hence the use of circular polarization in this case.

$$\begin{array}{llll} \gamma_1 & g[15] & \mathcal{G}_{1,1} & \gamma_4 \quad g[13] \quad 5\mathcal{B}^{(2)}_{2,1} \\ \gamma_2 & g[1] & \mathcal{B}_{1,1} & \gamma_5 \quad g[27] \quad 5\mathcal{G}^{(2)}_{2,1} \\ \gamma_3 & g[12] & 5\mathcal{B}^{(1)}_{2,1} & \gamma_6 \quad g[20] \quad \mathcal{G}^{(1)}_{2,1} \end{array} \tag{5.61}$$

Certain other measurements allow certain parameters to be tuned with measurement errors $O(1)$; in particular, measuring the parameters γ_1 and γ_2 with errors $O(1)$ allows the tuning respectively of $x_e(-\tau)$ and $y_e(-\tau)$ (which respectively measure the size of the static magnetic field in the x and the y direction where the electric field is ramping from zero) each with error $O(1)$. In this tune it is necessary to increase the value of k_ϵ from 66 to 67; the shift of $k_\epsilon + k_\beta$ from even to odd is required to access the terms needed.

Increasing the value of k_ϵ, and hence the value of the electric field, will change the atomic trajectory but will not change the values of the remnant magnetic fields at the entrance to plates, which can be zeroed and will remain zeroed when the electric field is lowered again so that k_ϵ returns to its standard value of 66. The measurements needed to measure γ_1 and γ_2 are

(a)	(b)	(c)	(d)	(e)	(f)	(g)	(h)	(i)	(j)	(k)	(l)
γ_1	z	Π	x	θ	z	Σ	...	...	θ_+	k odd	$\lvert\theta\rvert = \pi/2$
γ_2	z	Π	x	θ	z	Σ	...	...	θ_-	k odd	$\lvert\theta\rvert = 1.03224$

(5.62)

Other measurements isolate other parameters γ_3, γ_4, and γ_5 that in general represent certain integrals over the motional and static magnetic fields and so can contribute electric-field odd systematics to a measurement of an electron EDM. All these parameters cancel in a measurement of an electron EDM, so while the following operations measure each with a systematic error $O(1)$, it is not necessary to tune them; however knowing what they are and being able to bound them is an important fall-back. We do not trouble to measure γ_6 because it represents a positive definite integral with little useful information. The operations needed to measure the parameters are

(a)	(b)	(c)	(d)	(e)	(f)	(g)	(h)	(i)	(j)	(k)	(l)
γ_3	z	Π	x	θ	z	Σ	...	...	$\theta_+\Sigma_-E_+$	...	$\lvert\theta\rvert = \pi/2$ (or 0)
γ_4	z	Π	x	θ	z	Σ	...	...	$\theta_+\Sigma_-E_-$	...	$\lvert\theta\rvert = \pi/2$ (or 0)
γ_5	z	Π	x	θ	z	Σ	...	...	$\theta_-\Sigma_-$	...	$\lvert\theta\rvert = \pi/4$

(5.63)

Note that in measuring γ_3 and γ_4 one has to chop the sign of the electric field E.

It is not necessary to improve any of the four parameters in the initial tune of Eq. (5.59) from magnitudes $O(1)$ to $O(2)$ to measure an electron EDM with a systematic error $O(3)$, but it is easy to do. As it happens, once $x_e(-\tau)$ and $y_e(-\tau)$ have been reduced using the tune of Eq. (5.62) to be $O(1)$, simply repeating the tunings of Step 1 reduces the errors in measuring α_x, α_y and b to $O(2)$. Even with $x_e(-\tau)$ and $y_e(-\tau)$ reduced to be $O(1)$, there remains however an error of $O(1)$ in measuring a; however a single linear combination of the previous observable for a, recorded for a pair of magnitudes for the angle θ, call them θ_1 and θ_2, tunes a to zero with a sharply improved error of $O(3)$, so that all four original parameters of Eq. (5.59) have errors at least $O(2)$. The the two measurements of a required are

(a)	(b)	(c)	(d)	(e)	(f)	(g)	(h)	(i)	(j)	(k)	(l)
$a(1)$	x	Π	x	θ	x	Σ	...	...	$\theta_-\Sigma_-$	...	$\lvert\theta_1\rvert = 0.69967$
$a(2)$	x	Π	x	θ	x	Σ	...	...	$\theta_-\Sigma_-$	...	$\lvert\theta_2\rvert = 1.28115$

(5.64)

and the linear combination that isolates a is

$$a = -.232433\, a(1) + 1.094080\, a(2) + O(3) \tag{5.65}$$

Once the errors in the four parameters of the initial tune are of $O(2)$, we can refine the errors on other measurements. The following pair of measurements reduce the error in measuring $x_e(-\tau)$ and $y_e(-\tau)$ respectively each from $O(1)$ to $O(2)$. (It is not necessary to improve these from $O(1)$ to do an electron EDM measurement with an error of $O(3)$, but it can nonetheless be done straightforwardly.) Only a single measurement is required to isolate γ_1 with an error of $O(2)$:

(a)	(b)	(c)	(d)	(e)	(f)	(g)	(h)	(i)	(j)	(k)	(l)
γ_1	z	Π	x	θ	z	Σ	$\ldots$	$\ldots$	θ_+	k odd	$\lvert\theta\rvert = 0.70845$

(5.66)

However, two measurements are required to isolate γ_2, for example

(a)	(b)	(c)	(d)	(e)	(f)	(g)	(h)	(i)	(j)	(k)	(l)
$\gamma_2(1)$	z	Π	x	θ	z	Σ	$\ldots$	$\ldots$	θ_-	k odd	$\lvert\theta_1\rvert = 0.50000$
$\gamma_2(2)$	z	Π	x	θ	z	Σ	$\ldots$	$\ldots$	θ_-	k odd	$\lvert\theta_2\rvert = 1.03224$

(5.67)

when the linear combination that isolates γ_2 is

$$\gamma_2 = 6.700199\, \gamma_2(1) - 1.498090\, \gamma_2(2) + O(2)\ . \tag{5.68}$$

As indicated in Eq. (B.17), the addition of two measurements of γ_2 with errors $O(2)$ will measure the value of α_z, the rotation by static magnetic fields from state preparation to the point of the effective step-function jump of the electric field, with an error of $O(1)$.

We can refine the measurements on some parameters that we will ultimately contrive to cancel in a measurement of an electron EDM; in principle we do not need to improve these even to $O(1)$, so measuring them with systematic error $O(2)$ is certainly unnecessary but is straightforward. We have the measurements

(a)	(b)	(c)	(d)	(e)	(f)	(g)	(h)	(i)	(j)	(k)	(l)
$\gamma_3(1)$	z	Π	x	θ	z	Σ	$\ldots$	$\ldots$	$\theta_+\Sigma_-E_+$	$\ldots$	$\lvert\theta\rvert = 0$
$\gamma_3(2)$	z	Π	x	θ	z	Σ	$\ldots$	$\ldots$	$\theta_+\Sigma_-E_+$	$\ldots$	$\lvert\theta\rvert = \pi/4$

(5.69)

$$\gamma_3 = -7.29600\, \gamma_3(1) + 4.68712\, \gamma_3(2) + O(2)\ , \tag{5.70}$$

and

(a)	(b)	(c)	(d)	(e)	(f)	(g)	(h)	(i)	(j)	(k)	(l)
$\gamma_4(1)$	z	Π	x	θ	z	Σ	$\ldots$	$\ldots$	$\theta_+\Sigma_-E_-$	$\ldots$;	$\lvert\theta\rvert = 0$
$\gamma_4(2)$	z	Π	x	θ	z	Σ	$\ldots$	$\ldots$	$\theta_+\Sigma_-E_-$	$\ldots$;	$\lvert\theta\rvert = \pi/4$

(5.71)

$$\gamma_4 = -7.29600\, \gamma_4(1) + 4.68712\, \gamma_4(2) + O(2)\ . \tag{5.72}$$

To measure γ_5 efficiently, it is most helpful to vary the frequency of the analysis laser between states of different total spin F' within the $7P_{3/2}$ manifold; the measurement needed is described by

(a)	(b)	(c)	(d)	(e)	(f)	(g)	(h)	(i)	(j)	(k)	(l)
$\gamma_5(1)$	z	Π	x	θ	z	Σ	$\ldots$	$\ldots$	$\theta_-\Sigma_-$	$\ldots$	$\lvert\theta\rvert = \pi/4$, laser to $F' = 5$
$\gamma_5(2)$	z	Π	x	θ	z	Σ	$\ldots$	$\ldots$	$\theta_-\Sigma_-$	$\ldots$	$\lvert\theta\rvert = \pi/4$, laser to $F' = 4$

(5.73)

$$\gamma_5 = -2.96341\, \gamma_5(1) - 1.08200\, \gamma_5(2) + O(2)\ . \tag{5.74}$$

The scheme already described of measuring b with error $O(2)$ measures, when the electric field is reversed, an electron EDM with error $O(2)$; however there are four systematic effects that enter at $O(2)$ and tuning

and bounding all of them to get a systematic error that is net $O(3)$ is awkward. By tipping in the horizontal plane the axes of laser propagation with respect to the z axis we can cancel two of these four errors outright: these two errors enter because of the presence of nonzero amplitudes in the initial state for being in the states $\big|51\big\rangle$ and $\big|5,\,-1\big\rangle$, and the tipping makes those amplitudes zero.

We therefore define a laser axis $u(\lambda)$ where the unit vector u is the result of rotating a unit vector in the $+z$ direction by an angle λ about the y axis, where $|\lambda| < \pi/2$. Thus u lies in the horizontal (z-x) plane, and $u\cdot\hat{z} > 0$. If a laser that is linearly polarized propagates parallel to u, then the polarization vector lies in a plane perpendicular to u, and its orientation can be described by its angular position in that plane with respect to that vector v_λ in that plane that is in the z-x plane and has a positive projection onto the unit vector $\hat{z}$; the angle will be positive if the angle represents a rotation of that vector about the axis u that is positive according to the usual right-hand rule. To measure b with the maximum cancellation of systematics, we will wish to have lasers that can propagate parallel to either $u(+\lambda)$ or $u(-\lambda)$, with $|\lambda| = 0.28925$. The orientation of the lasers and their axes of linear polarization are shown in Fig. 5.4.

Once we are using lasers that propagate along the axes $u(\pm\lambda)$ and not along the z axis, there remain only the two systematic errors described in Eq. (5.5) and Fig. 5.5. As described there, one of these systematics will have been reduced to a negligible magnitude by the previous tune of $y_e(-\tau)$, and the other can be canceled because it and the effect of an electron EDM depend differently on the angle of linear polarization of the preparation laser. The linear combination of data that isolates the electron EDM is

(a)	(b)	(c)	(d)	(e)	(f)	(g)	(h)	(i)	(j)	(k)	(l)
$b(1)$	u_λ	Π	v_λ	θ	u_λ	Π	v_λ	0	$\theta_-\lambda_+$	...	$\lvert\lambda\rvert = 0.28925,\ \lvert\theta\rvert = 0.21381$
$b(2)$	u_λ	Π	v_λ	θ	u_λ	Π	v_λ	0	$\theta_-\lambda_+$	...	$\lvert\lambda\rvert = 0.28925,\ \lvert\theta\rvert = 0.69076$

(5.75)

$$b = 0.38315\,b(1) + 0.32386\,b(2) + O(3)\ . \tag{5.76}$$

The claim that the error in measuring an electron EDM is $O(3)$ depends on tuning four parameters—a, b itself, α_y, and y_e—to each be $O(1)$, which should not be difficult, as the system of tunings permits the error in each of these to be reduced to $O(2)$.

An error of $O(3)$ suffices to measure an electron EDM of our target sensitivity of $\mathbf{1.3\cdot 10^{-50}\,C\cdot m}$. We are confident that the scheme of cancellation will work to that order because the **scheme we have described actually works to one order beyond that, to O(4)**: provided the gradient y_1 (see Eq. (5.55)) in the vertical component of the magnetic field at the entrance of the electric field plates can be controlled to be of $O(1)$, then provided the previous four parameters can indeed be tuned to have errors $O(2)$, then the error in the electron EDM is of $O(4)$.

Of course, the possibility of realizing a cancellation of systematic errors at the extraordinarily low level of $O(4)$ within some model of an apparatus raises the question of what phenomena that model may overlook. We have for example assumed the laser polarizations to be perfect—purely linear or purely circular, as needed, and if linear, with an angle of polarization we can specify exactly. Having a polarization that is slightly elliptical will not change the fact that for the various transitions in use there will be a single dark state into which an atom will be pumped, but it will make that state contain undesired superpositions of states. Just as for the magnetometer described in Figures 3.10 and 3.11, in all cases of seeking to measure a small parameter because of these undesired superpositions one might well see a nonzero signal even if the parameter in question were strictly zero. Just as for the magnetometer, however, errors due to undesired superpositions can be canceled to leading order by taking the signal and subtracting the calibration signal obtained when the state analysis is timed to occur immediately after state preparation, before the atoms have traveled more than a few microns or have had any time for their atomic state to evolve. Such a subtraction can and should be carried out for every measurement in Eq. (5.59) through Eq. (5.76).